ASSESSMENT OF QUANTIZATION ARTIFACTS IN SDR AND HDR AND CNN-BASED CORRECTION

Edern Le Bot, Tania Pouli[1]

b<>com, Advanced Media Content Lab, Rennes, France

ABSTRACT

Most video contents are encoded using 8 bits per color channel, offering 256 possible values for each component. This has been sufficient for most traditional uses, but with the increased adoption of high dynamic range (HDR) technologies, standard dynamic range (SDR) content, may be up-converted to HDR, leading to an amplification of certain artifacts. Quantization artifacts in particular, taking the form of false contours, may become more visible after luminance expansion, especially in bright image areas. To correct such artifacts, debanding methods first aim at distinguishing between real image edges and contours due to quantization, and follow by filtering steps to correct them. Different criteria of visibility may be employed, but in all cases, the images are considered as they are. Nevertheless, when converting to HDR, if banding is corrected as a pre-process, the visibility of false contours should be assessed with this conversion in mind. To this end, in this work, we perform a series of user studies to assess different debanding approaches both in SDR and up-converted HDR images, exploring how the visibility of banding changes with luminance. We then discuss how CNN-based approaches could be extended to consider banding visibility in the context of luminance expansion.

INTRODUCTION

Color in digital images and video is represented using a limited number of distinct values, depending on the number of bits used (bit-depth). Traditionally, each color channel is encoded using 8 bits, however the increase in display capabilities, both in terms of display size and luminance levels means that smooth variations of color may lead to visible quantization steps, where changes between two subsequent values create an artificial edge or contour Figure 1. This kind of artifact is known as banding and it significantly affects the visual quality of images.

The increasing adoption of high dynamic range (HDR) technologies makes this issue more critical today. Existing, standard dynamic range (SDR) content is often up-converted to HDR, which is achieved by stretching or redistributing the luminance information of the image in order to extend its dynamic range. Whether this is achieved through global functions [1], [2] or local filters [3]–[5], a side effect of such conversions is that artifacts in the original image may be amplified. Solutions for reducing the visibility of such artifacts are therefore necessary.

[1] Contact: tania.pouli@b-com.com

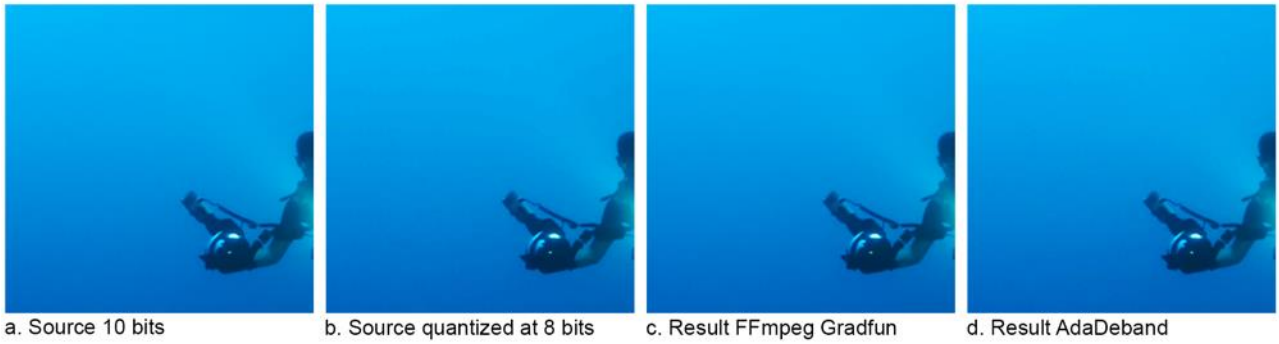

Figure 1: Example of banding and correction results (here shown with 30% contrast increase for visualization)

Several approaches exist to treat banding artifacts, generally consisting of two steps: locating false contours and potentially analyzing their characteristics, followed by a filtering step to correct them [6], [7]. The first step is necessary to ensure that only contours due to quantization are filtered, while real image edges and textures are preserved. A more detailed overview of different banding methods is given in the following section, but we observe that despite the extensive volume of work addressing this issue, the detection and localization of banding is typically based on an assessment of visibility, which in turn depends both on the image content itself but also on how the image is viewed

In the case of SDR to HDR conversions, it might not always be feasible to correct banding after luminance expansion, especially when such expansion depends on the target display luminance for example. In such scenario, it would be desirable to correct banding prior to expansion, but with knowledge of how the visibility of such artefact might be affected by the conversion and the target viewing conditions.

To address this challenge, in this work, we first aim to understand how luminance expansion affects the visibility of banding through a series of user tests. First, we evaluate the effectiveness of several existing debanding methods on a variety of SDR images. We then assess whether banding becomes more visible after up-conversion to HDR, evaluating the robustness of different correction approaches to this kind of transformation. Finally, we discuss how the predictive power of neural networks could be employed to correct banding as a pre-process prior to luminance expansion, while predicting the visibility of the false contours in the final viewing conditions.

BACKGROUND

To remove false contours in images, two general approaches may be followed depending on the goals of the correction. Different filters can be employed to reduce the visibility of false contours, while maintaining the bit-depth of the image, or alternatively, if the goal is to extend the bit-depth of the image, correction of banding can be performed simultaneously, taking advantage of the increased number of intensity steps of the new bit-depth.

In the simplest case, bit-depth extension from a low bit-depth L to a higher bit-depth H may be performed using simple bit manipulations, such as zero-padding, where a number $n = H - L$ of zeros is appended in the least significant bit (LSB) positions of the H bit-depth image, or multiplication by an ideal gain (MIG), where values in the L bit-depth image are multiplied by a fixed factor $m = \frac{2^H - 1}{2^L - 1}$ to obtain a H bit-depth image [8]. A slightly more

complex strategy is bit-replication, where instead of padding the $\lceil n \rceil$ LSB with zeros, the $\lceil n \rceil$ most significant bits (MSB) are copied to the $\lceil n \rceil$ LSB positions of the higher bit-depth image [8].

The above discussed approaches lead to an increase in bit-depth but do not offer corresponding visual improvements. To reduce the visibility of banding, while increasing the image bit-depth, Mittal et al. employ a classification approach where candidate values in the new higher bit-depth are characterized according to local neighborhood values a minimum risk strategy is employed for selecting the best candidate [9]. In an alternative solution [10], using an adaptive local filtering approach, the image bit-depth is first increased and contour artefacts are then reduced by applying a low pass filter to smooth areas.

When the goal is the reduction of the visibility of banding without an associated increase in bit-depth, methods cannot rely on the additional levels offered by the increased bit-depth to mask the appearance of false contours. Instead, contours are generally broken by the addition of well-controlled noise or dithering. To avoid modifying areas without banding, typically the first step is to detect where banding occurs. Bhagavathy et al. employ a multi-scale analysis to localize and characterize banding [6]. A probabilistic dithering step then follows to perturb pixel intensities in a local neighborhood of the appropriate scale, reducing the visibility of false contours. Although this approach can accurately find false contour, it boasts a heavy computational cost.

Baugh et al. [11] also employ dithering to reduce the visibility of banding, but propose a novel ‘banding index’ metric to quantify and localize banding in images, which aims to detect smooth regions. Using an RGB-based segmentation to detect large blocks of uniform values, a banding mask can be created, which guides subsequent filtering and dithering. Other efforts have been made to produce banding visibility metrics. Wang et al. [12] proposed a metric considering zero-gradient (homogeneous) connected edges as candidate banding edges: the length and neighborhood edge coherence of previously found edges is then assessed to produce a banding visibility map. Nevertheless, this kind of edge detection is very sensitive to edge noise. Tandon et al. [13] take a similar approach as [6] and make use of a banding confidence map extracted at multiple spatial frequencies with a fixed neighborhood size, which are then pooled together to produce a banding index. The authors also attempt to reduce the computational cost of the solution of Bhagavathy et al. [6] by fixing a set of hyper-parameters. In an alternative solution, Lee et al. make use of directional contrast features to apply an adaptive directional smoothing filter [14].

More accurate predictions about the visibility of contours can be performed by considering properties of visual perception, particularly luminance and chromatic contrast sensitivity (CSF) and visual masking effect [15]. Huang et al. [16] first compute a false contour candidate (FCC) map, by removing smooth regions and textured areas, taking advantage of above mentioned visual masking effect. Then pixels are selected according to their gradient profile in the previously found FCC pixels normal contour direction. Tu et al. similarly extract candidate banding edges by gradient thresholding and morphological operations, and then incorporate simple models of luminance and texture masking in their BBAND approach to remove detected edges that are likely to not be visible [17]. In [7], they further employ their proposed BBAND index to guide a filter-based banding correction method. To better match visual perception of banding, Denes et al. [18] consider a more complete model of chromatic contrast sensitivity [19], and make use of spatial-frequency components of the quantization error function to predict chromatic banding.

More recently, deep learning has been employed for correcting banding artifacts and extending image bit-depth. Among those methods, BitNet [20] is trained on pairs of source images and images with reduced bit depth with the aim of performing color reconstruction as well as quantization artefact suppression. BitNet produces effective results for low (3/4 bit) bit-depth conversion, however for higher bit-depth scenarios, e.g. 8 to 10-bit conversions, the proposed network would likely have to be retrained. Zhao et al. employ a two-layer residual network-based approach to treat both flat and non-flat areas appropriately [21]. Other attempts have also been made to perform bit depth extension using deep learning methods with multiple architectures. Punnapurath et al. [22] made a review of existing works, and proposed a new method, which was shown to outperform prior work.

Although the problems of both bit-depth extension and removal of false contours are not new, the majority of methods focus on use cases where source images are encoded in relatively low bit-depths. Further, in all cases described, the visibility of banding is assessed based on a direct evaluation of pixel values and relations, with no consideration of the encoding of the image. Implicitly, methods assume that images are SDR and used statistics and thresholds are designed accordingly. Nevertheless, contrast sensitivity – a feature often used to assess visibility of banding – depends on luminance, as such we might imagine that knowing the display luminance as well as the encoding (EOTF) of the image might have a significant effect on how banding is perceived. To this end, we assess banding visibility in both SDR and HDR conditions and explore directions for extending existing models to consider these aspects in their assessment of banding severity.

VISIBILITY OF BANDING

Several methods aim at detecting false contours that are likely to be visible. The criteria used may rely on low-level image statistics and thresholds [9] or on more complete perceptual models that consider contrast sensitivity [18]. Nevertheless, little data exists from subjective evaluations of banding artifacts.

To evaluate banding visibility in SDR and HDR conditions, as well as the effectiveness of different correction approaches, we perform a series of user studies, where for a selection of images, banding and image quality are assessed for several debanding methods, outlined in Table 1.

Method	Title
ADB	Adaptive Debanding Filter [7]
ADBd	Adaptive Debanding Filter with dithering [7]
FFDB	FFmpeg ‘deband’ filter
FFG	FFmpeg ‘gradfun’ filter
SRC	Source uncorrected image

Table 1: Compared debanding methods

In the first study, SDR images corrected with the selected methods are evaluated, providing a baseline. Then, to evaluate how robust these correction methods are against luminance expansion, we convert the processed images to HDR, targeting different peak luminance levels, using the SDR to HDR conversion solution developed by b<>com[2]. The up-converted HDR images are then used in a second subjective study. A detailed description of the stimuli and the experimental procedure used is given in the following.

[2] https://b-com.com/en/process/adaptive-hdr-converter

Stimuli

To provide realistic conditions, images were chosen from the YT-UGC video dataset[3], which contains typical user-generated videos for several categories, varying from sports, to music concerts, to animation and so on. For each video, an associated banding score is provided, computed using the perceptual metric of Wang et al. [12] discussed previously. For our studies, HD resolution videos were considered, and a selection[4] was made according to a combination of visual inspection and the provided banding score, selecting videos where banding was visible. The selected frames can be seen in Figure 2.

To further challenge the tested methods, we considered two possibilities. One option was to artificially increase quantization artifacts through bit-depth reduction, as was proposed by Kapoor et al. [23] in the construction of their banding dataset. The second option considered was to re-encode the videos using more aggressive compression settings, therefore amplifying banding and other compression artifacts. We opted for the latter option, as in our view represents a more realistic scenario and better corresponds with typical artifacts that may be encountered, especially in the use case of SDR to HDR expansion, where 6-bit or lower bit-depth sources are unlikely to be encountered.

In total, 10 video sequences were selected. Individual representative frames were extracted from each sequence, and each selected frame was processed with the chosen debanding methods (see Table 1). Together with the uncorrected source frames, 5 alternatives were thus included for each image, for a total of 50 stimuli for the first study.

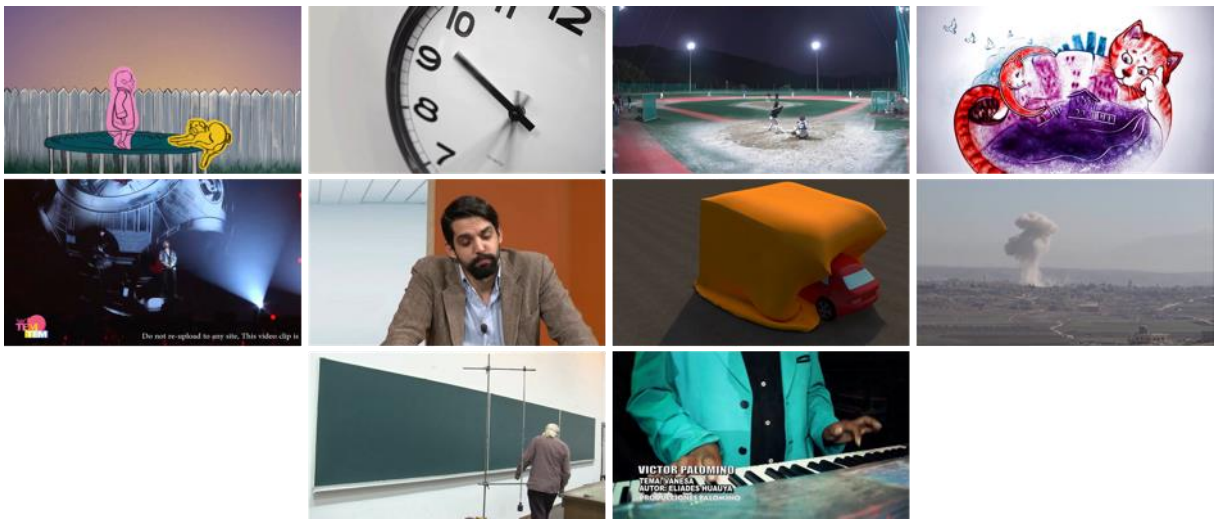

Figure 2: Selected frames from YT-UGC dataset.

For the second study, several peak luminance levels were considered when converting to HDR to assess whether the visibility of banding is affected by the content luminance. To keep the experiment duration reasonable, a subset of the debanding methods was used in this case. Specifically, in addition to the uncorrected images (SRC), the best two methods were selected following the results of the first study, namely the FFmpeg ‘gradfun’ filter (FFG) and the full adaptive debanding filter approach, including the dithering post-process

[3] https://media.withyoutube.com/

[4] Selected sequences from the YT-UGC dataset: Animation_1080P-3dbf, Animation_1080P-6ec0, LiveMusic_1080P-2930, LiveMusic_1080P-6b1c, NewsClip_1080P-2eb0, Animation_1080P-18f5, MusicVideo_1080P-16e6, Sports_1080p-19d8, NewsClip_1080P-7816, Lecture_1080P-238b

[7]. The number of different scenes considered was also reduced, keeping the 5 images where banding was more visible.

Experimental Procedure

The experiments were carried out on a calibrated Sony BVM X300 display, set to SDR mode (2.4 gamma, BT.709 color space), with a 100 cd/m^2 peak luminance for the first study, and set to HDR mode using the PQ EOTF and BT.2020 color space for the second study. In both cases ambient lighting was low.

To reduce potential order effects (due to participants becoming more familiar with the task or certain images, or due to fatigue), each participant saw a random permutation of the 50 stimuli in the SDR study. An image presenting natural (1/f) noise was shown after each stimulus. In the HDR study, a somewhat different procedure was chosen as different luminance levels were considered: stimuli were presented in blocks of increasing luminance (203 cd/m^2, followed by 600 and 1000 cd/m^2). For each luminance level, the order of methods was randomized, as well as the overall order in which image blocks were presented.

Participants were asked to rate each image they saw in terms of visibility of banding (VIS), and overall image quality (QUAL). Both criteria were rated in a Likert-like 5-level scale, going from low (1) to high (5). No time limits were enforced, and participants chose a comfortable viewing distance but were allowed to approach the display for close inspection.

RESULTS

The goal of the described studies is primarily to assess how the visibility of banding changes with dynamic range expansion and how robust debanding methods are against that. The first study serves to obtain a baseline of the visibility of banding in SDR images and how different methods perform. The HDR study expands upon the findings of the first, exploring how banding visibility is affected by the luminance target in luminance expansion, and evaluating the robustness of debanding methods when used as a pre-process prior to SDR-HDR up-conversion.

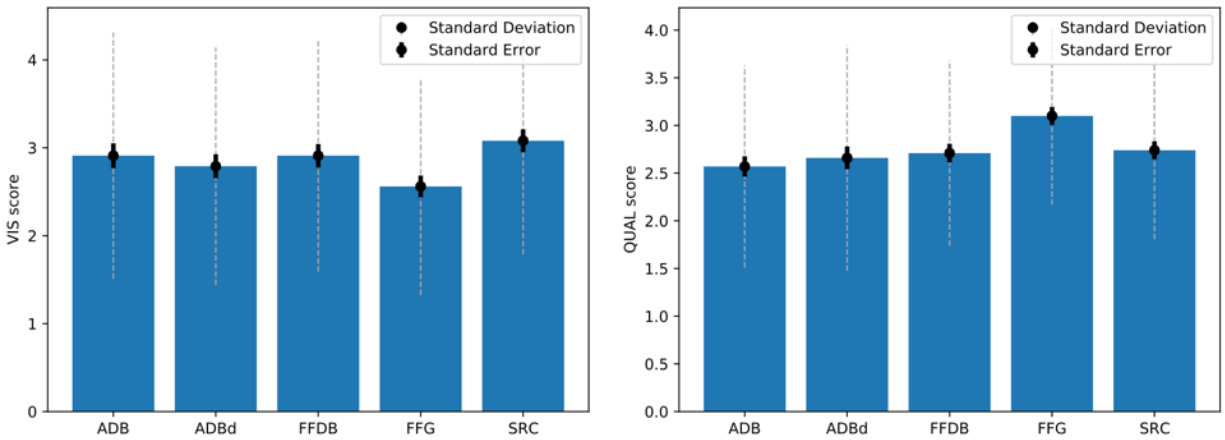

Figure 3: Mean VIS (left) and QUAL (right) scores for the tested methods for the SDR study, with standard deviation and standard errors shown.

SDR user study

In total, 10 participants took part in the first study. Aggregating the obtained scores for each method, we obtain mean visibility (VIS) and quality (QUAL) scores as shown in Figure 3. We observe that all correction methods lead to a lower banding visibility on average relative to the uncorrected sources, with FFG and ADBd showing the best performance.

	FFDB	ADB	ADBd	SRC	FFG
FFDB	1,00	0,59	0,96	0,36	0,07
ADB	0,59	1,00	0,57	0,70	0,02
ADBd	0,96	0,57	1,00	0,26	0,12
SRC	0,36	0,70	0,26	1,00	0,01
FFG	0,07	0,02	0,12	0,01	1,00

Table 2: T-test results between pairs of methods across all participants and images for the SDR user test VIS scores

To further analyze these differences, t-tests were performed for each method pair to assess whether their differences could be considered significant (Table 2). We can observe that FFG shows significant differences against SDR, FFDB and ADB ($p < 0.05$), while the results of FFG and ADBd are not statistically different, despite the observed differences in mean. All other results are not significantly different considering even the rather conservative threshold of $p < 0.1$.

We might expect these differences to amplify with a larger pool of participants, however it is interesting to note that the majority of debanding methods are typically demonstrated in the context of banding due to low bit-depth corrections, while in our case a more realistic scenario was chosen where banding and compression artifacts are mixed.

All stimuli were evaluated not only for the visibility of banding (VIS) but also the overall image quality (QUAL), allowing us to assess how the two criteria relate. A Spearman correlation value of R = -0.34 was found, suggesting a weak negative correlation between them: as the visibility of banding increased, the overall perceived image quality decreased.

HDR user study

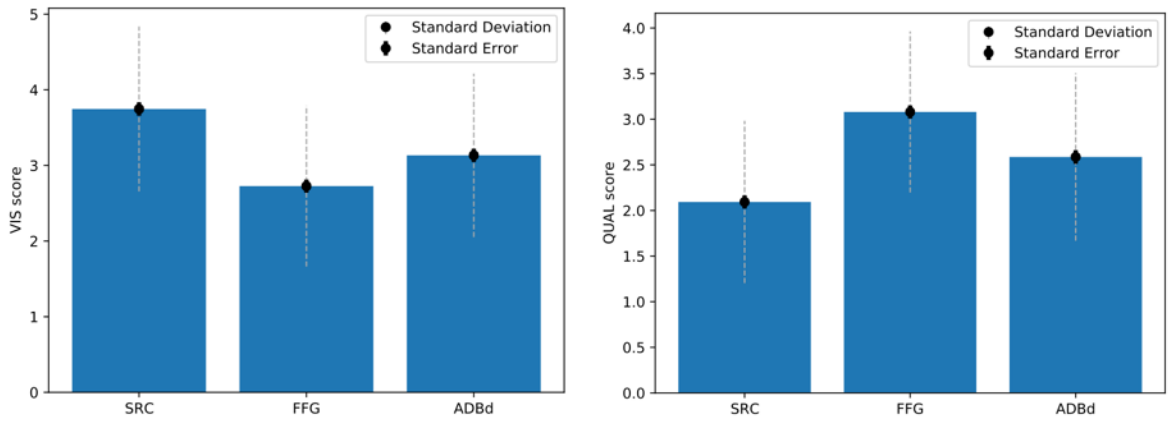

Figure 4: Mean VIS and QUAL scores for the tested methods aggregated across the three peak luminance conditions of the HDR study.

Based on these preliminary results, to assess the effect of luminance expansion on the visibility of banding, we chose to focus on the best two methods identified, namely ADBd and FFG. 10 participants took part in this second study. A similar analysis was performed for the HDR study as described in the previous section to assess the performance of the

different methods. Figure 4 shows the aggregated VIS and QUAL means for the tested methods. From these results, we observe that the tested methods overall maintain the same relative ordering as in the SDR study, with FFG outperforming ADBd, and both methods leading to lower banding visibility and higher image quality relative to the source. T-test results for each method pair show that these differences are significant (Table 3).

To better understand how luminance affects the visibility of banding, mean VIS and QUAL scores were also computed for each peak luminance level, shown in Figure 5. Banding was deemed less visible in the lower luminance condition (203 cd/m^2), however results for the 600 and 1000 cd/m^2 conditions were very similar. T-tests between pairs of luminance levels are shown in Table 4, confirming the above observations.

	SRC	FFG	ADBd
SRC	1,000	0,000	0,000
FFG	0,000	1,000	0,001
ADBd	0,000	0,001	1,000

Table 3: P-values between method pairs for VIS scores from the HDR study

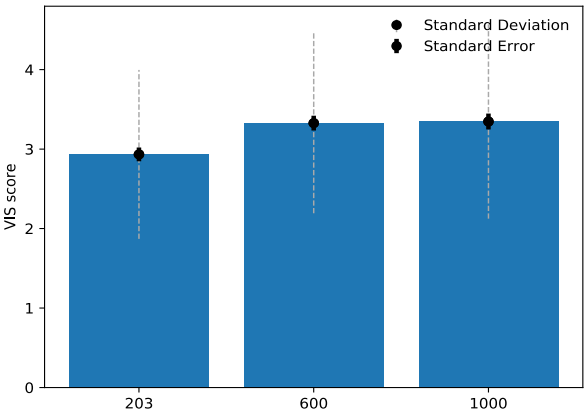

Figure 5: Mean VIS scores and errors for each luminance level.

	203	600	1000
203	1.00	0.006	0.006
600	0.006	1.00	0.88
1000	0.006	0.88	1.00

Table 4: T-test p-values comparing VIS scores for each pair of luminance values

Interestingly, this is consistent with the non-linear nature of light perception [24]. As an example, Figure 6 shows the relation between linear luminance the lightness channel taken from the CIELab perceptual color space, where it can be seen that as luminance levels increase, their perceptual distance compresses.

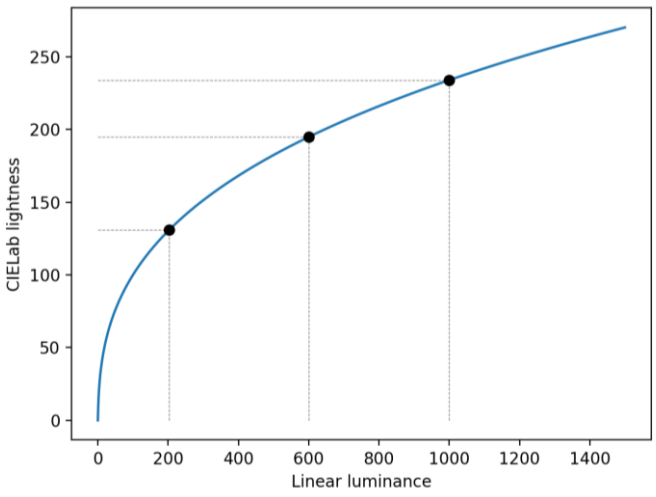

Figure 6: Luminance is perceived in a non-linear manner, compressing perceived differences as luminance levels increase.

To better understand how the luminance level used in the SDR to HDR expansion interacts with the different debanding methods, means were also grouped by method for each luminance level and vice versa, shown in Figure 7. In all cases, the 600 and 1000 cd/m^2 conditions were very close to each other, as was observed in the aggregated results. Further, the relative performance of the tested methods was consistent across luminance conditions. A two-way

ANOVA assessing both methods and luminance level conditions showed that both conditions lead to significantly different behaviors individually ($p < 0.0001$ both). Consistent with what can be observed in Figure 7, no interaction was found between the two conditions ($p = 0.9$).

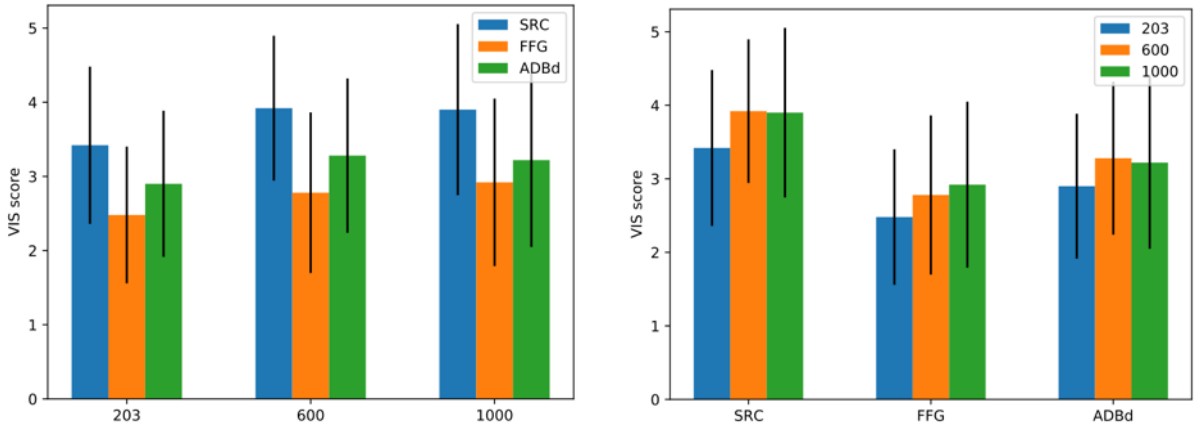

Figure 7: Detailed results grouping mean VIS scores by luminance (left) or method(right).

COMPARISONS WITH BANDING METRICS

As previously discussed, several metrics have been proposed for blind assessment of banding [12], [13], [17]. Here, we compare our findings with the predictions of the BBAND index [17], which also serves as a basis for the AdaDeband correction method [7].

We first computed the correlation of average VIS scores obtained from the SDR user study for each image and the corresponding BBAND prediction. Although the images used in our study are somewhat different to the banding scenario for which the BBAND index is optimized (low bit-depth), we find reasonable correlation when compared with the source images. This is consistent with the banding scores provided for each source sequence within the Youtube UGC dataset, which are computed using the perceptual metric of Wang et al. [12], leading to a Spearman R of 0.57 and a Pearson R of 0.53 when compared against our user scores. The BBAND index was less able to predict banding after different corrections were applied, despite users still perceiving banding artefacts (see Figure 3).

Comparing the BBAND predictions against our HDR findings for the up-converted HDR images (Table 5), we can observe that for higher luminance values, the banding index is better able to predict the presence of banding, while for the 203 cd/m^2 condition, no correlation is found. Perhaps surprisingly, a stronger correlation is found for the 600 and 1000 cd/m^2 HDR conditions than for the SDR source images. However, this be can possibly explained by the fact that luminance expansion tends to stretch the higher parts of the luminance distribution, exaggerating banding in bright areas.

	203	**600**	**1000**
Spearman	0,00	0,45	0,60
Pearson	-0,05	0,91	0,86

Table 5: Correlation between average VIS scores for HDR up-converted images with no correction at different luminance values and BBAND index.

DISCUSSION

The above presented studies raise several interesting observations. In the case of SDR images, the tested methods certainly show a positive effect in reducing the visibility of false contours and simultaneously increasing the perceived image quality. However, this effect was relatively minor in the type of images and artifacts that we selected, suggesting that debanding methods are perhaps less effective when banding is confounded with compression artifacts. It should nevertheless be noted that the pool of participants for our study was relatively small, and the observed effects would likely be strengthened with a larger number of participants.

Moving onto the HDR results, we note that no banding correction methods have been designed with HDR imagery and luminance expansion in mind to our knowledge. Whether explicitly stated or not, existing methods assume that content will be SDR and gamma-encoded, and have certain expectations in terms of how images are likely to be viewed. Nevertheless, if we consider contrast sensitivity, it is well-known that the luminance of the signal plays an important role [25].

Indeed, by examining how the results of the BBAND index correlate with the scores of our user study, we note that the peak luminance targeted during SDR to HDR expansion significantly changes how well such a metric can predict the presence of banding.

In our tests, debanding methods were used as a pre-process on the input to the SDR-HDR expansion, and had no knowledge of how the image luminance was expanded. As we saw though, the targeted peak luminance had a significant effect on how banding was perceived, irrespective of whether a correction was applied prior to expansion or not, suggesting that to effectively treat banding in the context of luminance expansion, the complete processing should be considered.

This can be achieved in two manners. HDR up-converted images could be treated with a debanding approach after expansion. Although no HDR-adapted debanding methods exist yet, a CSF-based solution could be developed incorporating a model such as the one proposed by Denes et al. [26] in the banding detection process. However, in many scenarios, it would be desirable to perform the debanding prior to luminance expansion, e.g. if content is converted to HDR on the client-side (TV, set-top box etc.), thus also ensuring that the source is of as high a quality as possible.

To that end, an interesting avenue for future work opens through recent developments in CNN-based bit-depth expansion and debanding. Networks such as BitNet [20] or the network of Zhao et al. [21] are trained on pairs of high and low bit-depth images to learn how to correctly reconstruct details lost due to quantization. Their ‘understanding’ of banding is therefore implicitly based on the differences between the two images, an approach which cannot be readily employed in the context of debanding prior to luminance expansion.

A potential solution can be found in [21], where Zhao et al. supplement their network with an external flat area detection, guiding how each image area should be treated. In a similar vein, such a network could be enriched with a banding detection block instead, itself trained to predict banding in SDR images through SDR-HDR pairs at different luminances through the help of a CSF model covering extended luminance levels. In this case, banding correction would take the more traditional form of detection followed by filtering, as is the case with most existing approaches, while at the same time taking advantage of the predictive power that a CNN can offer to accurately detect banding in SDR images with their ultimate HDR target in mind.

CONCLUSIONS

In this work, through a series of user studies, we evaluate the effectiveness of different debanding methods and explore how the visibility of banding changes with luminance, specifically in the context of SDR to HDR luminance expansion. Our findings suggest that the visibility of banding is amplified with luminance expansion and that false contour artifacts become increasingly visible with higher peak luminance. Current debanding methods are limited to SDR imagery, and are not sufficient for correcting banding artifacts if used as a pre-process prior to HDR up-conversion. To effectively address banding in this scenario, banding visibility would have to be assessed by considering not only the content of the SDR image but also how the final HDR image will be encoded and viewed, a task for which existing CNN-based debanding solutions could be extended, by explicitly considering banding visibility as determined by contrast sensitivity models.

REFERENCES

[1] B. Masia, A. Serrano, and D. Gutierrez, “Dynamic range expansion based on image statistics,” *Multimed. Tools Appl.*, no. August 2015, pp. 1–18, 2015, doi: 10.1007/s11042-015-3036-0.

[2] C. Bist, R. Cozot, G. Madec, and X. Ducloux, “Tone expansion using lighting style aesthetics,” *Comput. Graph.*, vol. 62, pp. 77–86, 2017, doi: 10.1016/j.cag.2016.12.006.

[3] F. Banterle, P. Ledda, K. Debattista, and A. Chalmers, “Expanding low dynamic range videos for high dynamic range applications,” *Proc. 24th Spring Conf. Comput. Graph.*, pp. 33–41, 2008, doi: 10.1145/1921264.1921275.

[4] A. G. Rempel and M. Trentacoste, “Ldr2Hdr,” *ACM Trans. Graph.*, vol. 26, no. 99, p. 39, 2007, doi: 10.1145/1239451.1239490.

[5] R. P. Kovaleski and M. M. Oliveira, “High-quality brightness enhancement functions for real-time reverse tone mapping,” *Vis. Comput.*, vol. 25, no. 5–7, pp. 539–547, 2009, doi: 10.1007/s00371-009-0327-3.

[6] S. Bhagavathy, J. Llach, and J. Zhai, “Multiscale probabilistic dithering for suppressing contour artifacts in digital images,” *IEEE Trans. Image Process.*, vol. 18, no. 9, pp. 1936–1945, 2009, doi: 10.1109/TIP.2009.2022293.

[7] Z. Tu, J. Lin, Y. Wang, B. Adsumilli, and A. C. Bovik, “Adaptive Debanding Filter,” *IEEE Signal Process. Lett.*, 2020, doi: 10.1109/LSP.2020.3024985.

[8] R. Ulichney and S. Cheung, “Pixel Bit-Depth Increase by Bit Replication,” vol. 1, no. 3.

[9] G. Mittal, V. Jakhetiya, S. P. Jaiswal, O. C. Au, A. K. Tiwari, and D. Wei, “Bit-depth expansion using minimum risk based classification,” in *2012 IEEE Visual Communications and Image Processing, VCIP 2012*, 2012, no. November, doi: 10.1109/VCIP.2012.6410837.

[10] C. H. Liu, O. C. Au, P. H. W. Wong, M. C. Kung, and S. C. Chao, “Bit-depth expansion by adaptive filter,” *Proc. - IEEE Int. Symp. Circuits Syst.*, vol. 1, no. 2, pp. 496–499, 2008, doi: 10.1109/ISCAS.2008.4541463.

[11] G. Baugh, A. Kokaram, and F. Pitié, “Advanced video debanding,” 2014, doi: 10.1145/2668904.2668912.

[12] Y. Wang, S. U. Kum, C. Chen, and A. Kokaram, “A perceptual visibility metric for banding artifacts,” in *Proceedings - International Conference on Image Processing, ICIP*, 2016, vol. 2016-Augus, pp. 2067–2071, doi: 10.1109/ICIP.2016.7532722.

[13] P. Tandon, M. Afonso, J. Sole, and L. Krasula, “CAMBI: Contrast-aware Multiscale Banding Index,” *arXiv Prepr.*, 2021, [Online]. Available: http://arxiv.org/abs/2102.00079.

[14] J. W. Lee, B. R. Lim, R. H. Park, J. S. Kim, and W. Ahn, “Two-stage false contour detection algorithm using re-quantization and directional contrast features and its application to adaptive false contour reduction,” *Dig. Tech. Pap. - IEEE Int. Conf. Consum. Electron.*, vol. 2006, pp. 377–378, 2006, doi: 10.1109/ICCE.2006.1598468.

[15] S. J. Daly and X. Feng, “Decontouring: prevention and removal of false contour artifacts,” 2004, doi: 10.1117/12.526937.

[16] Q. Huang, H. Y. Kim, W. J. Tsai, S. Y. Jeong, J. S. Choi, and C. C. J. Kuo, “Understanding and Removal of False Contour in HEVC Compressed Images,” *IEEE Trans. Circuits Syst. Video Technol.*, 2018, doi: 10.1109/TCSVT.2016.2607258.

[17] Z. Tu, J. Lin, Y. Wang, B. Adsumilli, and A. C. Bovik, “Bband Index: a No-Reference Banding Artifact Predictor,” *ICASSP, IEEE Int. Conf. Acoust. Speech Signal Process. - Proc.*, vol. 2020-May, pp. 2712–2716, 2020, doi: 10.1109/ICASSP40776.2020.9053634.

[18] G. Denes, G. Ash, H. Fang, and R. K. Mantiuk, “A visual model for predicting chromatic banding artifacts,” *IS T Int. Symp. Electron. Imaging Sci. Technol.*, vol. 2019, no. 12, 2019, doi: 10.2352/ISSN.2470-1173.2019.12.HVEI-212.

[19] K. J. Kim, R. Mantiuk, and K. H. Lee, “Measurements of achromatic and chromatic contrast sensitivity functions for an extended range of adaptation luminance,” 2013, doi: 10.1117/12.2002178.

[20] J. Byun, K. Shim, and C. Kim, “BitNet: Learning-Based Bit-Depth Expansion,” in *Lecture Notes in Computer Science (including subseries Lecture Notes in Artificial Intelligence and Lecture Notes in Bioinformatics)*, 2019, vol. 11362 LNCS, pp. 67–82, doi: 10.1007/978-3-030-20890-5_5.

[21] Y. Zhao, R. Wang, W. Jia, W. Zuo, X. Liu, and W. Gao, “Deep Reconstruction of Least Significant Bits for Bit-Depth Expansion,” *IEEE Trans. Image Process.*, vol. 28, no. 6, pp. 2847–2859, 2019, doi: 10.1109/TIP.2019.2891131.

[22] A. Punnappurath and M. S. Brown, “A Little Bit More: Bitplane-Wise Bit-Depth Recovery,” *arXiv*. 2020.

[23] A. Kapoor, J. Sapra, and Z. Wang, “CAPTURING BANDING IN IMAGES : DATABASE CONSTRUCTION AND OBJECTIVE ASSESSMENT,” *ICASP*, no. June, 2021.

[24] M. A. Abebe, T. Pouli, M.-C. Larabi, and E. Reinhard, “Perceptual Lightness Modeling for High-Dynamic-Range Imaging,” *ACM Trans. Appl. Percept.*, vol. 15, no. 1, pp. 1–19, 2017, doi: 10.1145/3086577.

[25] P. G. Barten, *Contrast Sensitivity of the Human Eye and Its Effects on Image Quality*. 2009.

[26] G. Denes, G. Ash, H. Fang, and R. K. Mantiuk, “A visual model for predicting chromatic banding artifacts,” *Electron. Imaging*, vol. 2019, no. 12, pp. 212-1-212–8, 2019.